Title

Computational design of ultrasensitive flexible peptide:receptor signaling complexes for enhanced chemotaxis

Authors

Jefferson RE[1], Oggier A[1], Fuglistaler A[1], Camviel N[2], Hijazi M[1], Rico Villarreal A[1], Arber C[2], Barth P[1, §]

Affiliation

1: Interfaculty Institute of Bioengineering, Ecole Polytechnique Federale de Lausanne, Lausanne, CH-1015, Switzerland and Ludwig Institute for Cancer Research Lausanne, Switzerland

2: Department of oncology UNIL-CHUV, University Hospital Lausanne (CHUV), University of Lausanne (UNIL) and Ludwig Institute for Cancer Research Lausanne, Switzerland

§ Correspondences should be addressed to:

Patrick Barth, Interfaculty Institute of Bioengineering, Ecole Polytechnique Fédérale de Lausanne, Lausanne, CH-1015, Switzerland, patrick.barth@epfl.ch

Abstract

Engineering biosensors that sensitively recognize specific biomolecules and trigger functional cellular responses is a holy grail of diagnostics and synthetic cell biology. Biosensor design approaches have mostly focused on binding structurally well-defined molecules. Coupling the sensing of flexible compounds to complex cellular responses would considerably expand biosensor applications, but remains challenging. We developed a computational strategy for designing highly sensitive receptor biosensors of flexible peptides. Using the method, we created ultrasensitive chemotactic GPCR:peptide pairs capable of eliciting potent chemotaxis in human primary T cells. Through mutual induced fit, our flexible structure design approach enhanced peptide contacts with binding and allosteric sites in the ligand pocket to achieve unprecedented signaling efficacy and potency. The approach paves the road for designing peptide-sensing receptors and expanding the biosensor toolbox for basic and therapeutic applications.

Designing biosensors with arbitrary input and output behaviors is a grand challenge of synthetic biology. Current approaches focus on engineering binding to structurally well-defined protein[1] and small-molecule chemical cues[2], and couple molecular recognition to synthetic optical reporters that are built-in modular biosensor scaffolds. While this strategy provides elegant solutions to the design of *in vitro* diagnostics, applications for *in vivo* detection and synthetic cell biology rely on coupling the molecular sensor to the precise activation and orchestration of complex intracellular signaling functions that often cannot be recapitulated *de novo*. Harnessing synthetic sensing to fine-tuned native signaling functions in a biosensor scaffold is limited by our poor mechanistic understanding of allosteric signal transduction and lack of techniques to rationally engineer these properties.

Peptides mediate close to 40 % of cell signaling functions through ubiquitous interactions with membrane receptors and soluble proteins[3,4]. Unbound peptide ligands are often partially disordered in solution, which challenges structure determination, and computational sampling of the vast conformational space. In contrast to rigid protein binders and small-molecule ligands, structural information on peptide binding is scarce and limits supervised training and validation of deep-learning[5–7] and physics-based[8] protein:peptide complex structure prediction approaches. The specific receptor:peptide engineering problem is further complicated by the high flexibility of both receptor and peptide ligand which through mutual induced fit often adopt a new conformation together to reach the active state and initiate signal transduction. The rational design of peptide-sensing receptors has not been reported to date.

Here, we describe and apply a computational strategy for engineering membrane receptors with high binding sensitivity to flexible peptide ligands and potent allosteric signal transduction responses across the membrane. Unlike previous work that only optimize binding and model receptors as rigid target structures[9], we build fully flexible receptor:peptide conformational ensembles that enable the precise modeling of signaling active states and the design of complexes with novel contact networks enhancing both binding sensitivity and allosteric response (**Figure 1A**). Through this approach, we aim to design custom-built modular biosensors that can link binding of a flexible peptide input signal to selective, fine-tuned and complex cellular responses through genetically encoded single-receptor

domains. We define this new class of biosensors as CaPSens, which stands for Conformationally-adaptive Peptide BioSensor.

To demonstrate this strategy, we designed ultrasensitive CaPSens of chemotactic peptides for reprogramming cellular migration (**Figure 1A**). Chemotactic peptides are attractive targets since directional movement of cells in response to gradient of these molecules (e.g. chemotaxis) is essential throughout biology and control over this represents one of the great challenges of synthetic cell biology. For example, efficient immune cell homing to cancer cells is one of the bottlenecks in modern immunotherapy[10–14]. Hence, these therapeutic approaches would benefit from engineered cytotoxic lymphocytes with enhanced chemotaxis towards tumor sites. Since cell migration relies on the precise orchestration of diverse intracellular activities, we build and carve novel synthetic sensing properties onto natural chemotactic receptor scaffolds for optimal interfacing with the complex intracellular machinery of eukaryotic cells that mediate chemotaxis[15–18].

Molecular recognition between flexible peptide and signaling receptors usually involves significant structural rearrangements of both molecules through conformational selection (i.e. selection from an ensemble of unbound conformations) and induced fit (i.e. conformational changes occurring upon binding) effects. Therefore, we reasoned that an effective method for evolving novel interaction networks optimizing peptide recognition and long-range allosteric response should explore a vast conformational binding space through sampling of peptide conformational ensemble but also extensive structural relaxation of peptide bound receptor complexes. Our computational strategy was developed with these ideas in mind and proceeds in the following main steps (**Figure 1B**): (i) building hybrid transmembrane (TM) scaffolds in active signaling conformation using structure pieces from distinct chemotactic receptors to generate diverse possible biosensor templates; (ii) docking of fully flexible peptides onto the active-state receptor scaffold binding sites to identify possible interacting conformations from the large diversity of unbound peptide structures; (iii) filter and diversify peptide positions to generate a peptide-bound receptor ensemble representative of the vast conformational binding space and diverse networks of contacts; (iv) *de novo* loop rebuilding of the biosensor scaffold

to accommodate peptide-bound structure; (v) relax the resulting receptor:peptide complex structure to populate the most optimal binding conformations through mutual induced fit effects; (vi) computational selection of novel binding and allosteric contact networks at the receptor:peptide interface followed by structural relaxation; (vii) experimental validation of selected designs using a battery of cell-based functional assays; (viii) experimentally guided refinement of receptor:peptide conformational ensemble to improve modeling accuracy; (ix) design of highly sensitive receptor:peptide super-agonist pairs for enhanced chemotaxis.

As a proof of concept, we modeled and designed peptide ligand agonists starting from the N-terminal partially unstructured agonist region of the chemokine CXCL12, which promotes strong activation of the CXCR4 receptor[19,20]. To build and evolve CaPSens scaffolds sensing CXCL12-derived peptides, we selected structural parts from the chemokine receptor family. In absence of a CXCR4 structure in the signaling active form, biosensor templates were assembled from local structures of CXCR4 in the inactive form and the structure of the homologous viral chemokine receptor US28 bound to CX3CL1 (4XT1)[21], the only active-state chemokine receptor structure available at the time of modeling. Our modeling stage (steps i-iv) yielded 9 major peptide-bound biosensor scaffold structures that provided starting templates for a first round of computational design (**Figure 1B**). In the following, we name designs by the approach (Cdes for combinatorial design, Ldes for point mutant library design, CLdes for combined Cdes and Ldes solutions) and design generation (1 and 2).

Since the first two N-terminal positions of CXCL12 are critical for activation and even conservative mutations can lead to drastic signaling defects[22–24], we focused our initial computational design on improving the binding of the sensor to positions 3 through 8 of the CXCL12-derived peptide (P3 through P8), up to the CXC motif. Our design strategy focuses on the first-shell of residues in contact with the peptide ligand, thus we expect to improve binding, however, we also inevitably reinforce previously identified[23,25–27] or uncover new allosteric sites on the pocket surface. The first round of calculations yielded a novel binding hotspot motif with improved interfacial contact density between the

TM1/7 interface and P3 of the peptide as well as new interactions with the allosteric position 1.39 (**Figure 2A,B**). We validated the peptide binding and signaling properties of the Cdes1 receptor in HEK cells using cell based assays reporting G-protein $G\alpha_i$ activation and Ca^{2+} mobilization that are triggered by native chemokine receptors and known to be crucial for chemotactic responses[15,28]. Consistent with the prediction, the designed receptor displayed enhanced sensitivity to CXCL12 (**Figure 2C,D**). We built upon the initial success of the Cdes1 design by further optimizing the binding interface upstream of P3. A second binding hotspot motif was selected between P7 of CXCL12 and 3 positions lining the beta hairpin of the receptor second extracellular loop (ECL2) (**Figure 2A,B**). Combining the 2 designed motifs into the Cdes2 receptor led to substantially enhanced potency in calcium mobilization (3.1-fold over WT) and $G\alpha_i$-coupling (3.2-fold over WT) (**Figure 2E,F**). To rapidly identify additional binding and activating motifs, we then rationally created and screened a computationally guided library of variants built from our initial ensemble of receptor:peptide models. Each variant was designed by mutating a single predicted peptide binding and/or allosteric residue and assayed for calcium mobilization and $G\alpha_i$ coupling (**Figure 2G**). Activating point mutations were identified at novel sites on TM1, TM3 and ECL2 and assembled into a library-selected combination (Ldes) receptor variant (**Figure 2A,B**). The Ldes design was considerably more sensitive than the starting CXCR4 WT scaffold with close to 11-fold enhanced $G\alpha_i$ potency and 120 % of WT efficacy (**Figure 2G**). We next thought to combine the initial designed binding hotspot motifs from Cdes2 with these new activating sites. Additive effects were observed when combining the most activating mutation with the Cdes2 design and led to a CLdes sensor that had the second-most potent and sensitive $G\alpha_i$ response (more than 9-fold increase over WT) against WT CXCL12 in our designs (**Figure 2H**). These results indicate that our approach can readily design highly sensitive sensors of the WT CXCL12 chemokine derived peptide by optimizing both binding and signaling determinants.

We next sought to create selective receptor:peptide pairs by designing novel peptide super-agonists. Such synthetic sensor-response systems would provide orthogonal solutions for reprogramming cellular activity and bypass the high level of binding promiscuity inherent to native

receptors. From our computational models, we identified 2 sites P3 and P7 on the peptide scaffolds where novel and stronger contacts with the receptor binding pocket could be designed. A designed Leu at P7 further optimized packing complementarity with the binding hotspot motif of the Cdes2 design, enhanced $G\alpha_i$ efficacy by 130 % of the designed sensor while decreasing the overall response of the WT receptor scaffold (**Figure 3A**). At position P3, our calculations identified bulky aromatic residues predicted to complement the TM 1/2 pocket interface of the designed sensors, leading to extremely powerful activating effects. Specifically, the Ldes:V3Y peptide pair displayed more than 80-fold enhanced potency and a 125 % increase in efficacy compared to the WT receptor:peptide pair (**Figure 3B,D**). The CLdes:V3Y-Y7L peptide pair boosted both potency and efficacy by more than 100-fold and 134 %, respectively (**Figure 3C,D**). These results demonstrate the power of our computational approach for engineering novel synthetic receptor:peptide pairs with highly sensitive binding properties and potent downstream signaling.

We next assessed whether our ultra-sensitive CaPSens also elicited a cell migratory phenotype with concomitant sensitivity upon detection of chemokines. Chemotaxis results from the complex orchestration of multiple intracellular pathways that control receptor oligomerization, cell motility, polarity, adhesion, following receptor-mediated G-protein activation triggered by the sensing of chemokine proteins[15–18] (**Figure 3E**). Such validation represents a stringent test of our ability to leverage molecular design for cell engineering and reprogram complex cellular behaviors in responses to environmental cues. We transduced primary human T cells with selected designed sensors and measured their migration against gradients of full-length WT or engineered chemokines incorporating the designed N-terminal peptide tail. Chemotaxis was measured using boyden chambers in which cells can migrate across a porous membrane towards a reservoir containing chemoattractant. Migratory indices were measured as a function of the fold-migration over a no-chemoattractant control for each transduced donor. T cells transduced with the Cdes2, Ldes and CLdes designs displayed up to almost 5-fold increased migration towards 100 nM wild-type CXCL12. At this level of chemoattractant, WT CXCR4 promoted around 1.5-fold enhanced migration when compared to the no-attractant controls (**Figure 3F**).

Our engineered CaPSens also boosted T cell migration by up to 4.5-fold when exposed to designed chemokines (**Figure 3F**). The enhanced cellular migration demonstrates that the designed molecular signaling properties leading to ultra-high sensitivity of our sensors translate into the intended reprogramming of cell phenotypes. It also indicates that our strategy focusing on the flexible peptide region of the chemokine is generalizable to the design of biosensors responding to full-length chemoattractants. Overall, our results suggest that engineered receptors could trigger migration towards cancer-prone sites at longer distances with shallower chemokine gradients when compared to native chemotactic systems. Our designed CaPSens:hyper-agonist peptide pairs open the door to bringing cell migration under exogenous and spatiotemporal control, providing a promising new synthetic cell biology tool.

The diverse designed receptor-peptide agonist pairs offer a unique opportunity to assess the structural underpinnings of receptor:peptide binding and agonism. Unlike most binding interfaces between globular proteins, our designs displayed considerable structural adaptation to sequence changes. On the peptide side, we observed large shifts in peptide backbone and side-chain conformations except for the two most buried and constrained P1 and P2 sites (**Figure 4A**). Structural remodeling of the receptors was also noticeable and best quantified using a volumetric analysis of the peptide binding site. Cross-sectional areas at different depths of the binding pocket highlighted significant conformational adaptation of the binding surface (by up to 25 % at certain cavity depths) in response to the different peptide conformation and sequences (**Figure 4B**). We confirmed our models with molecular dynamics simulations, which recapitulated 75 to 91 % of the modeled contacts. When mapped onto a 3D map of the structure-function relationship (**Figure 4C**), the three most sensitive designed pairs occupy subspaces that are far apart in both receptor binding site and peptide conformation dimensions. These observations suggest the existence of multiple solutions for designing potent peptide biosensors with optimal sensing and signaling response. Owing to substantial backbone movements, the peptide may access an ensemble of microstates whose occupancy can be readily shifted via changes in sequence and/or receptor shape. The receptor binding pocket displays also

significant structural plasticity and can accommodate diverse peptide conformations. This concurrent structural adaption on both sides of the interface underlies a design process by mutual induced fit that enables the formation of diverse novel networks of productive binding and allosteric contacts, respectively modulating the potency and efficacy of the signaling response (**Figure 4D**). In fact, each of the highly sensitive biosensor-peptide pair displayed specific patterns of potency and efficacy determining contacts. For example, through rewired P7 interactions with the ECL2 loop in the CLdes-V3Y-Y7L peptide design pair, the P7 position was unlocked from its native conformation enabling the peptide to populate a more efficacious microstate through significant backbone shifts. Our results support a view of receptor-peptide sensing where the inherent plasticity of the binding interface enables the efficient adaptation of contact networks in response to even limited shifts in sequence space. Modeling and designing receptor-peptide interactions as conformationally dynamic complexes allows us to exploit this hallmark and readily evolve novel functional pairs.

To our knowledge, the computational design of peptide binding receptors with highly optimized binding and allosteric signaling functions is unprecedented. Most biosensor design approaches have focused on engineering protein domains for optimal recognition of structurally well-defined molecules. By targeting flexible and structurally uncharacterized peptides, our design platform significantly expands the range of molecules that can be detected by biosensors. Unlike approaches that rely on multi-domain sensor reconstitution upon ligand sensing, our method optimizes the coupling between molecular recognition and allosteric response in a single protein domain within the restricted design space of the ligand pocket interface and can generate CaPSens with unprecedented dynamic and sensitive responses. Carving biosensors into versatile GPCR scaffolds offers key additional advantages. GPCRs can now be engineered to trigger a wide range of intracellular functions through reprogrammed coupling to diverse effectors including G-proteins and arrestins[29,30]. Alternatively, inserting fluorescent protein domains into GPCR scaffolds enables fast and direct optical detection of ligand molecules[31]. As such, our approach paves the road for a wide range of synthetic biology, diagnostics and therapeutic

applications that would benefit from sensor systems that trigger complex cellular outputs or enable direct highly sensitive detection of chemical cues.

Figures

Fig 1. **Modeling and design strategy of Conformationally-adaptive Peptide BioSensor (CaPSens).** (**A**) Schematic of targeting binding and activation residues for design of chemotactic receptors with enhanced responses towards peptide attractants. The peptide ligand (blue) makes specific contacts with receptor pocket residues that are classified as drivers of binding (orange) or activation (green). Through design, receptor:peptide connectivity can be rewired to promote binding (top), activation, or both (bottom) to ultimately reprogram the cell migratory response. (**B**) Pipeline of the design strategy involving receptor:peptide modeling, rational design, experimental validation, and selection of final model ensemble.

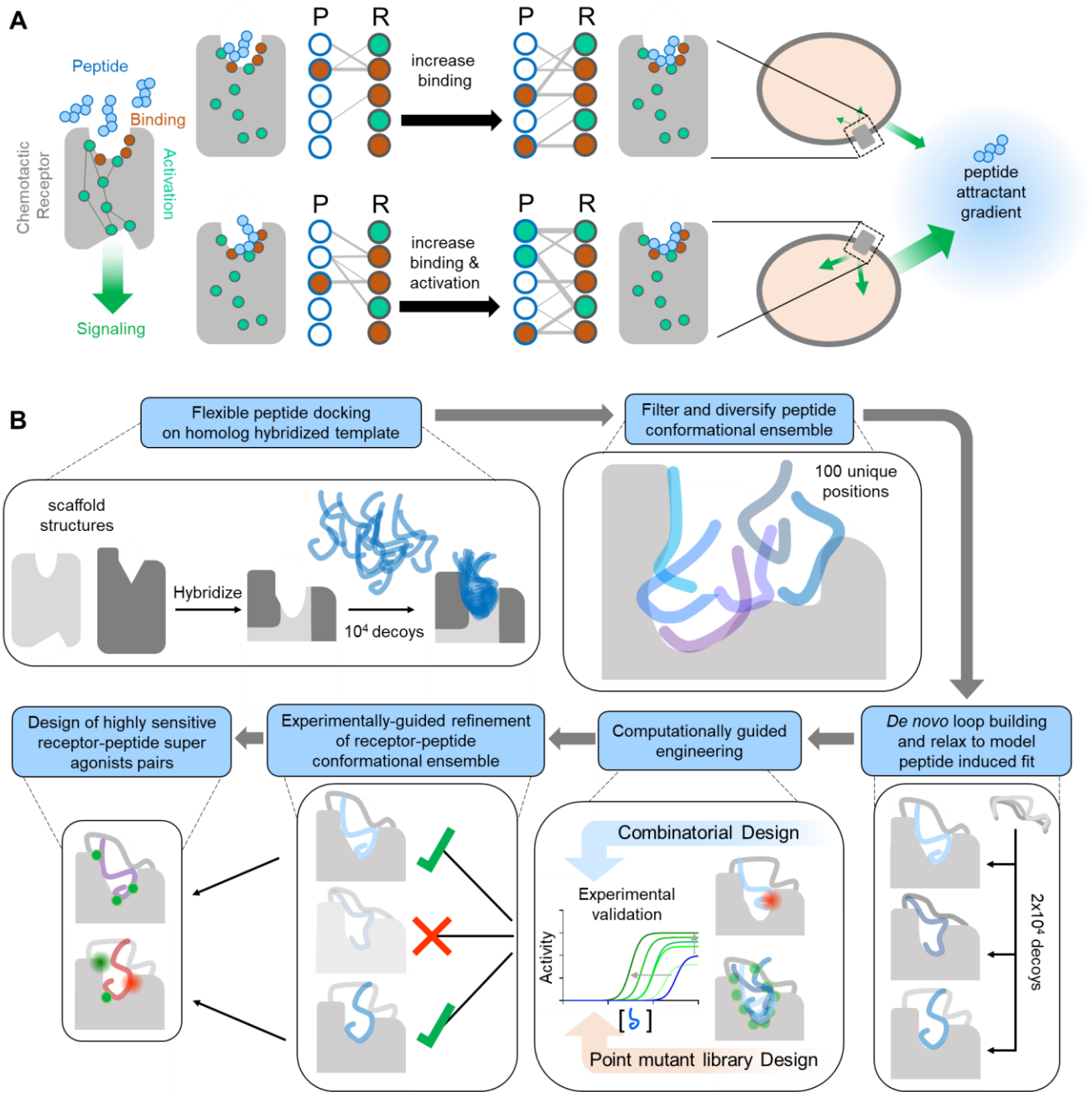
A
Peptide
Binding
Chemotactic Receptor
Activation
Signaling
P
R
increase binding
increase binding & activation
peptide attractant gradient
B
Flexible peptide docking on homolog hybridized template
scaffold structures
Hybridize
10⁴ decoys
Filter and diversify peptide conformational ensemble
100 unique positions
De novo loop building and relax to model peptide induced fit
2x10⁴ decoys
Computationally guided engineering
Combinatorial Design
Experimental validation
Activity
Point mutant library Design
Experimentally-guided refinement of receptor-peptide conformational ensemble
Design of highly sensitive receptor-peptide super agonists pairs

Figure 2. Design of receptor:peptide binding sites for enhanced sensing. (**A**) Primary sequence mapping of receptor residues targeted for design. (**B**) Location of the designed residues (shown in sticks) mapped onto the biosensor peptide binding site backbone structure (shown in cartoon). The peptide is represented as a gray-colored surface. (**C-H**) Peptide-induced cell signaling responses of designed receptors measured through $G\alpha_i$ activation and calcium release: $G\alpha_i$ BRET of Cdes1 design (**C**), Cdes2 design (**D**), and library-screened mutations (**E**). Calcium mobilization of Cdes1 design (**F**) and Cdes2 design (**G**). Effect of single-point library mutations in Cdes2 design background (**H**).

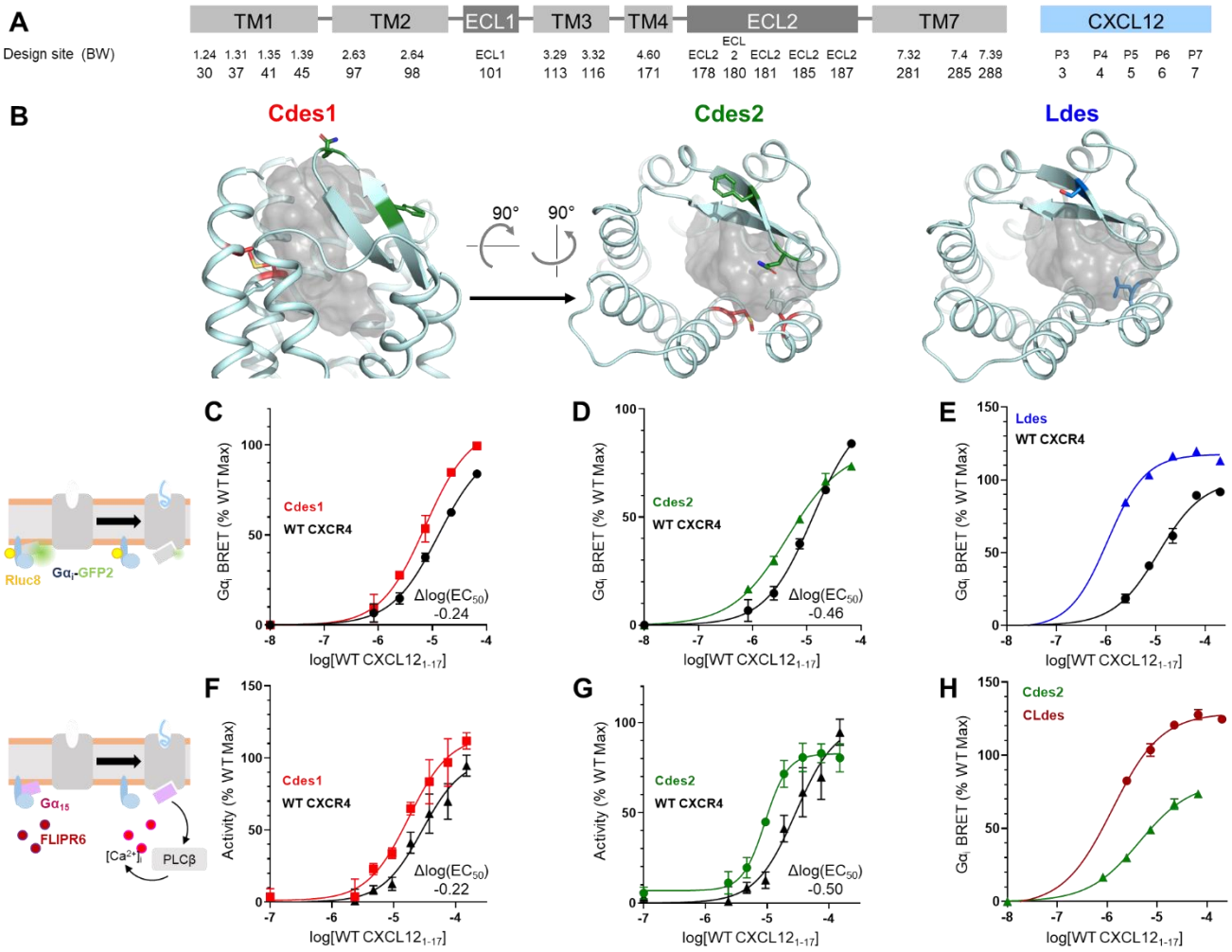

Figure 3. **Design of highly-sensitive and chemotactic receptor:peptide pairs. A-D.** Shifts in sensitivity (95 % confidence interval of dose response curve fits) and maximum activity (fitted value) for various receptor-peptide pairs involving the following designed peptides: (**A**) CXCL12 Y7L variant, (**B**) CXCL12 V3 substitutions, (**C**) CXCL12 V3Y/W-Y7L. (**D**) Changes in potency and efficacy across three separate experiments (each n=3), s.e.m. plotted. (**E**) Schematic of boyden chamber migration assay of T cells transduced with engineered receptors and (**F**) migratory responses of transduced primary T cells towards full-length chemokine. Bars are colored according to the transduced CXCR4 variant, and individual points are colored according to the CXCL12 variant. *: p⩽0.05, **: p⩽0.01, ***:p⩽0.001, ****:p⩽0.0001.

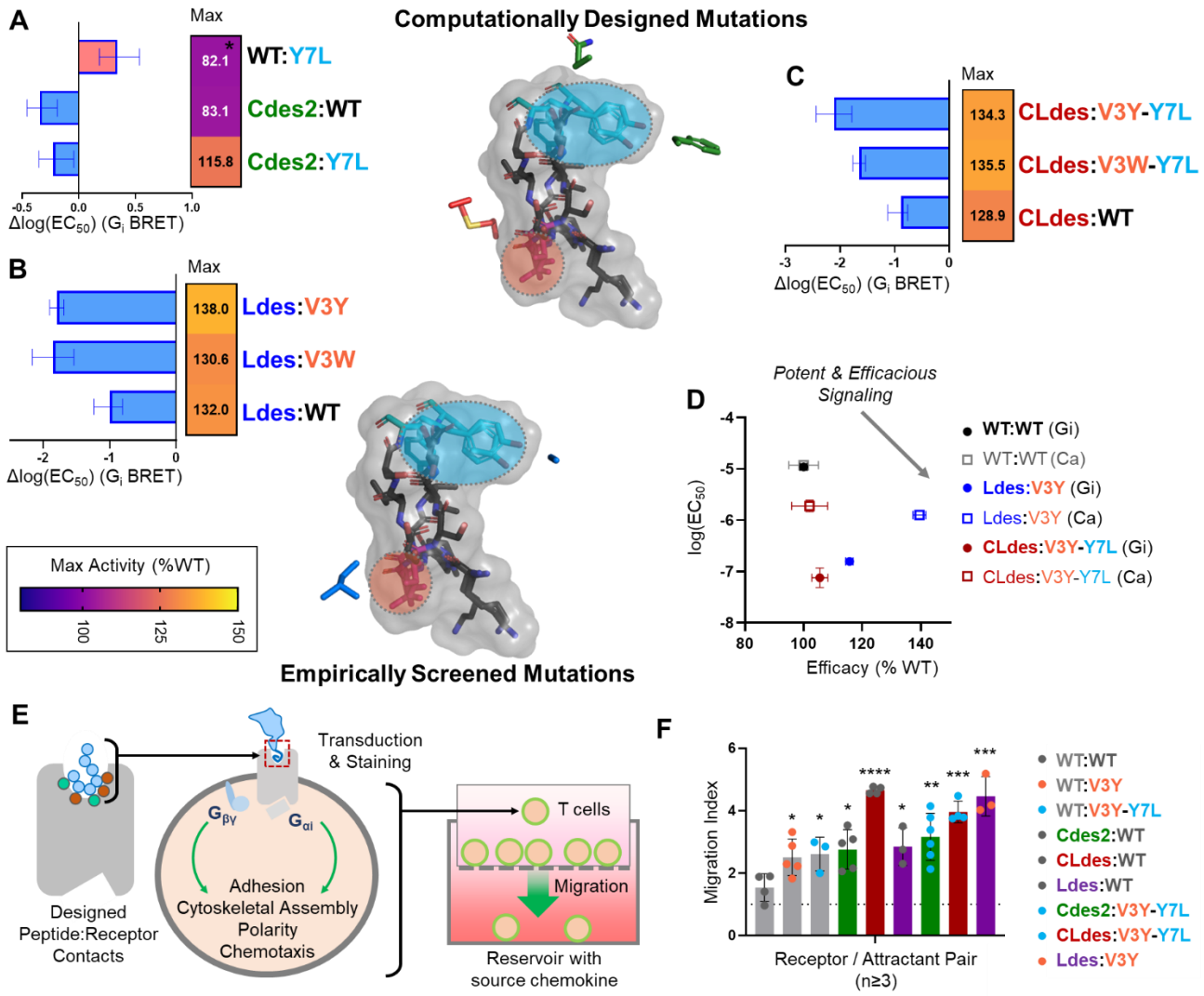

Figure 4. **High level of structural adaptation at the designed peptide-receptor binding interface.** (**A**) Cross-sectional views of receptor cavity at CXCL12.P3 depth for the following pairs: WT CXCR4:WT CXCL12, Ldes CXCR4:V3Y, Cdes2 CXCR4:Y7L CXCL12, and CLdes CXCR4:V3Y-Y7L CXCL12. The solvent accessible boundary at the P3 peptide position is shown in yellow. (**B**) Receptor cavity cross-sections at 3 distinct peptide positions mapped onto the WT CXCR4: WT CXCL12 structure (left). Cross-sectional area of the binding cavity as a function of cavity depth for distinct peptide-receptor pairs (right). (**C**) 3D map of structure-function relationship. Activity shifts from WT of individual receptor-peptide pairs (z-axis for potency and bars colored according to maximal activity) are plotted as a function of conformational shifts of the peptide (y-axis: calculated by Principal Component Analysis on bound peptide ensembles) and conformational shifts of the receptor binding pocket (x-axis: calculated by cross-sectional area). (**D**) Peptide:receptor contributions to potency and efficacy were derived from previous mutagenesis studies[23,25–27] and this study for the WT CXCR4:CXCL12 and designed complexes, respectively. Residue connectivity inferred from direct contacts in the final WT CXCR4:WT CXCL12 and CLdes CXCR4:V3Y-Y7L CXCL12 structures.

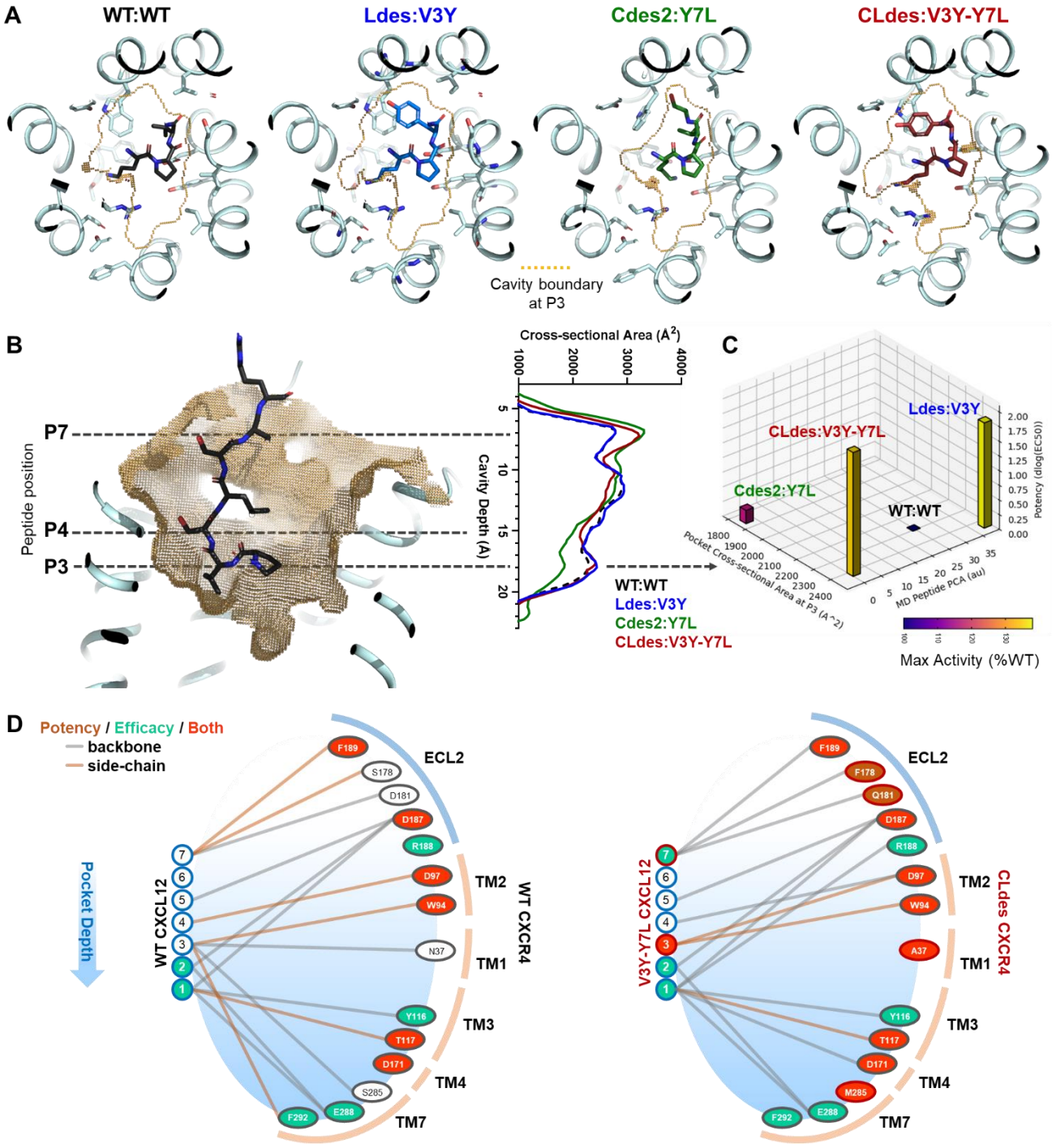
A
WT:WT
Ldes:V3Y
Cdes2:Y7L
CLdes:V3Y-Y7L
Cavity boundary at P3
B
P7
P4
P3
Peptide position
Cross-sectional Area (Å²)
Cavity Depth (Å)
WT:WT
Ldes:V3Y
Cdes2:Y7L
CLdes:V3Y-Y7L
C
Ldes:V3Y
CLdes:V3Y-Y7L
Cdes2:Y7L
WT:WT
Potency (dlog(EC50))
Pocket Cross-sectional Area at P3 (A^2)
MD Peptide PCA (au)
Max Activity (%WT)
D
Potency / Efficacy / Both
backbone
side-chain
Pocket Depth
WT CXCL12
WT CXCR4
ECL2
TM2
TM1
TM3
TM4
TM7
V3Y-Y7L CXCL12
CLdes CXCR4

Acknowledgements

We thank the Barth lab members for helpful discussions. Funding: R.E.J. is supported by a Marie Curie Postdoctoral Fellowship (H2020 fund 588412). A.R. is supported by an EPFLglobaLeader doctoral fellowship. P.B. is supported by a Swiss National Science Foundation grant (SNSF grant 31003A_182263), Swiss Cancer Research (KFS-4687-02-2019), funds from EPFL and the Ludwig Institute for Cancer Research. C.A. receives funding from Swiss Cancer Research KFS-4542-08-2018-R, Stiftung für Krebsbekämpfung, the Department of oncology UNIL CHUV, University of Lausanne, Lausanne University Hospital, and the Ludwig Institute for Cancer Research. Author contributions: R.E.J. and P.B. designed the study; R.E.J. and A.F. developed and tested the method, R.E.J. and M.H. performed calculations; R.E.J., A.O. and A.R. performed the experimental validation of the designs; N.C. transduced human primary T cells; C.A. supervised the T cell transduction and analyzed results; R.E.J. and P.B. analyzed, interpreted results and wrote the manuscript. Competing interests: P.B. holds patents and provisional patent applications in the field of engineered T cell therapies and protein design. C.A. holds patents and provisional patent applications in the field of engineered T cell therapies. All other authors declare no competing financial interest.

References:

1. Quijano-Rubio, A. *et al.* De novo design of modular and tunable protein biosensors. *Nature* 1–9 (2021) doi:10.1038/s41586-021-03258-z.
2. Glasgow, A. A. *et al.* Computational design of a modular protein sense-response system. *Science* **366**, 1024–1028 (2019).
3. London, N., Raveh, B. & Schueler-Furman, O. Peptide docking and structure-based characterization of peptide binding: from knowledge to know-how. *Current Opinion in Structural Biology* **23**, 894–902 (2013).
4. Petsalaki, E. & Russell, R. B. Peptide-mediated interactions in biological systems: new discoveries and applications. *Current Opinion in Biotechnology* **19**, 344–350 (2008).
5. Jumper, J. *et al.* Highly accurate protein structure prediction with AlphaFold. *Nature* 1–11 (2021) doi:10.1038/s41586-021-03819-2.
6. Baek, M. *et al.* Accurate prediction of protein structures and interactions using a three-track neural network. *Science* (2021) doi:10.1126/science.abj8754.
7. Lei, Y. *et al.* A deep-learning framework for multi-level peptide–protein interaction prediction. *Nat Commun* **12**, 5465 (2021).
8. Ciemny, M. *et al.* Protein–peptide docking: opportunities and challenges. *Drug Discovery Today* **23**, 1530–1537 (2018).
9. Alam, N. & Schueler-Furman, O. Modeling Peptide-Protein Structure and Binding Using Monte Carlo Sampling Approaches: Rosetta FlexPepDock and FlexPepBind. in *Modeling Peptide-Protein Interactions* 139–169 (Humana Press, New York, NY, 2017). doi:10.1007/978-1-4939-6798-8_9.
10. Vignali, D. & Kallikourdis, M. Improving homing in T cell therapy. *Cytokine & Growth Factor Reviews* **36**, 107–116 (2017).
11. Sackstein, R., Schatton, T. & Barthel, S. R. T-lymphocyte homing: an underappreciated yet critical hurdle for successful cancer immunotherapy. *Laboratory Investigation* **97**, 669–697 (2017).
12. Garetto, S., Sardi, C., Morone, D. & Kallikourdis, M. Chemokines and T Cell Trafficking into Tumors: Strategies to Enhance Recruitment of T Cells into Tumors. in *Defects in T Cell Trafficking*

and Resistance to Cancer Immunotherapy 163–177 (Springer, Cham, 2016). doi:10.1007/978-3-319-42223-7_7.

13. Slaney, C. Y., Kershaw, M. H. & Darcy, P. K. Trafficking of T Cells into Tumors. *Cancer Res* **74**, 7168–7174 (2014).
14. Melero, I., Rouzaut, A., Motz, G. T. & Coukos, G. T-Cell and NK-Cell Infiltration into Solid Tumors: A Key Limiting Factor for Efficacious Cancer Immunotherapy. *Cancer Discov* **4**, 522–526 (2014).
15. Surve, C. R., To, J. Y., Malik, S., Kim, M. & Smrcka, A. V. Dynamic regulation of neutrophil polarity and migration by the heterotrimeric G protein subunits Gαi-GTP and Gβγ. *Sci. Signal.* **9**, ra22–ra22 (2016).
16. Martínez-Muñoz, L. *et al.* Separating Actin-Dependent Chemokine Receptor Nanoclustering from Dimerization Indicates a Role for Clustering in CXCR4 Signaling and Function. *Molecular Cell* **70**, 106-119.e10 (2018).
17. Chandan, N. R., Abraham, S., SenGupta, S., Parent, C. A. & Smrcka, A. V. A network of Gαi signaling partners is revealed by proximity labeling proteomics analysis and includes PDZ-RhoGEF. *Science Signaling* (2022) doi:10.1126/scisignal.abi9869.
18. Swaney, K. F., Huang, C.-H. & Devreotes, P. N. Eukaryotic Chemotaxis: A Network of Signaling Pathways Controls Motility, Directional Sensing, and Polarity. *Annual Review of Biophysics* **39**, 265–289 (2010).
19. Loetscher, P., Gong, J.-H., Dewald, B., Baggiolini, M. & Clark-Lewis, I. N-terminal Peptides of Stromal Cell-derived Factor-1 with CXC Chemokine Receptor 4 Agonist and Antagonist Activities. *J. Biol. Chem.* **273**, 22279–22283 (1998).
20. Szpakowska, M. *et al.* Different contributions of chemokine N-terminal features attest to a different ligand binding mode and a bias towards activation of ACKR3/CXCR7 compared with CXCR4 and CXCR3. *British Journal of Pharmacology* **175**, 1419–1438 (2018).
21. Burg, J. S. *et al.* Structural basis for chemokine recognition and activation of a viral G protein–coupled receptor. *Science* **347**, 1113–1117 (2015).

22. Jaracz-Ros, A. *et al.* Differential activity and selectivity of N-terminal modified CXCL12 chemokines at the CXCR4 and ACKR3 receptors. *Journal of Leukocyte Biology* **107**, 1123–1135 (2020).
23. Crump, M. P. *et al.* Solution structure and basis for functional activity of stromal cell-derived factor-1; dissociation of CXCR4 activation from binding and inhibition of HIV-1. *The EMBO Journal* **16**, 6996–7007 (1997).
24. Ziarek, J. J. *et al.* Structural basis for chemokine recognition by a G protein–coupled receptor and implications for receptor activation. *Sci. Signal.* **10**, eaah5756 (2017).
25. Wescott, M. P. *et al.* Signal transmission through the CXC chemokine receptor 4 (CXCR4) transmembrane helices. *PNAS* **113**, 9928–9933 (2016).
26. Kufareva, I. *et al.* Stoichiometry and geometry of the CXC chemokine receptor 4 complex with CXC ligand 12: Molecular modeling and experimental validation. *PNAS* **111**, E5363–E5372 (2014).
27. Thiele, S., Mungalpara, J., Steen, A., Rosenkilde, M. M. & Våbenø, J. Determination of the binding mode for the cyclopentapeptide CXCR4 antagonist FC131 using a dual approach of ligand modifications and receptor mutagenesis. *Br J Pharmacol* **171**, 5313–5329 (2014).
28. Arai, H., Tsou, C.-L. & Charo, I. F. Chemotaxis in a lymphocyte cell line transfected with C-C chemokine receptor 2B: Evidence that directed migration is mediated by βγ dimers released by activation of Gαi-coupled receptors. *PNAS* **94**, 14495–14499 (1997).
29. Young, M. *et al.* Computational design of orthogonal membrane receptor-effector switches for rewiring signaling pathways. *PNAS* **115**, 7051–7056 (2018).
30. Paradis, J. S. *et al. Computationally designed GPCR quaternary structures bias signaling pathway activation*. 2021.09.23.461493 https://www.biorxiv.org/content/10.1101/2021.09.23.461493v1 (2021) doi:10.1101/2021.09.23.461493.
31. Patriarchi, T. *et al.* Ultrafast neuronal imaging of dopamine dynamics with designed genetically encoded sensors. *Science* eaat4422 (2018) doi:10.1126/science.aat4422.